ELSEVIER

Journal of Organometallic Chemistry 488 (1995) 205–210

Journal of Organometallic Chemistry

# Donor–acceptor-based vinylidene and $\sigma$-acetylide complexes of ruthenium and osmium

Andrew J. Hodge [a], Scott L. Ingham [a], Ashok K. Kakkar [b], Muhammad S. Khan [a], Jack Lewis *[a], Nicholas J. Long [a], David G. Parker [c], Paul R. Raithby [a]

[a] *University Chemical Laboratory, Lensfield Road, Cambridge CB2 1EW, UK*
[b] *Department of Chemistry, McGill University, 801 Sherbrooke St. West, Montreal, Quebec H3A 2K6, Canada*
[c] *ICI Group R&T Affairs, P.O. Box 90, Wilton Centre, Middlesborough, Cleveland, TS 90 8JE, UK*

Received 26 August 1994

---

**Abstract**

The synthesis of vinylidene, *trans*-[(dppm)$_2$ClM=C=C(H)(R)]PF$_6$, and $\sigma$-acetylide complexes, *trans*-[(dppm)$_2$ClM–C≡C–R] (M = Ru, Os; dppm = bis(diphenylphosphino)methane, Ph$_2$PCH$_2$PPh$_2$; R = $p$-C$_6$H$_5$, $p$-C$_6$H$_4$–C$_6$H$_5$, $p$-C$_6$H$_4$–NO$_2$, C$_6$H$_3$-2-(CH$_3$)-4-NO$_2$, $p$-C$_6$H$_4$–CH$_3$), and a single-crystal X-ray determination of *trans*-[(dppm)$_2$ClRu–C≡C–C$_6$H$_4$-$p$-NO$_2$] are reported. The metal–phosphine fragment in these complexes acts as a donor and communicates with the *para*-substituted nitro acceptor group through the backbone. Such an interaction helps create a delocalized charge-transfer state from the donor to the acceptor.

*Keywords:* Ruthenium; Osmium; Vinylidene; Acetylide; Crystal structure

---

## 1. Introduction

Organic molecules with asymmetric $\pi$-electron delocalization along the backbone (e.g., **1**) have been shown to display interesting physical properties such as second-order non-linearity [1]. The basic requirements for large values of $\beta$ in a molecule are: (i) high donor and acceptor abilities of the substituents at *para* positions to each other, leading to asymmetric charge distribution; (ii) a pathway for $\pi$-conjugated electrons; and (iii) an optimized $\pi$-electron conjugation length between them. The interest in such molecules is heightened by the fact that the acentric assemblies with large values of bulk polarizabilities ($\chi^2$) are ideal candidates for a variety of materials applications. Substitution of organic donor/acceptor fragments in these molecules with appropriate organometallic fragments which introduce additional perturbations of the $\pi$-electron cloud by d$\pi$(metal)–p$\pi^*$(organic) interactions and contain low-lying charge transfer states, is an alternative way of optimizing the non-linear optical response of such systems. Such effects have been demonstrated recently [2] in organometallic complexes such as ($Z$)-{1-ferrocenyl-2-(4-nitrophenyl)ethylene} (**2**). The $\sigma$-acetylide complexes of transition metals that are asymmetrically substituted (e.g., **3**) constitute another class of complexes which have potential for second-order non-linear optics [3].

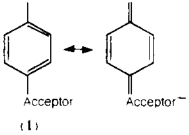

(1)

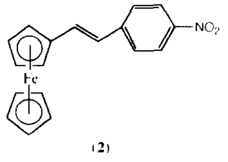

(2)

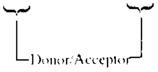

(3)

We report herein the synthesis of vinylidene and monoacetylide complexes of ruthenium and osmium in which the transition metal–phosphine fragments act as donors, *trans*-[(dppm)$_2$ClM=C=C(H)(R)]PF$_6$ and *trans*-[(dppm)$_2$ClM–C≡C–R] (M = Ru, Os; dppm = bis(diphenylphosphino)methane, Ph$_2$PCH$_2$PPh$_2$; R = $p$-C$_6$H$_5$, $p$-C$_6$H$_4$–C$_6$H$_5$, $p$-C$_6$H$_4$–NO$_2$, C$_6$H$_3$-2-(CH$_3$)-4-NO$_2$, $p$-C$_6$H$_4$–CH$_3$, and a single-crystal X-ray determination of the complex *trans*-[(dppm)$_2$ClRu–C≡C–C$_6$H$_4$-$p$-NO$_2$]. The osmium–vinylidene analogues are the first examples of such complexes.

---

* Corresponding author.

*SSDI* 0022-328X(94)00032-8

## 2. Results and discussion

The reactions of terminal acetylenes with Ru(II) and Os(II) complexes, $[MXL_n(C_5H_5)]$ (M = Ru, Os; X = Cl, Br; L = $PPh_3$, $Ph_2PCH_2PPh_2$, $Ph_2PCH_2CH_2PPh_2$) [4a,4b] have been the subject of much interest. Recently, Dixneuf et al. demonstrated that $RuCl_2(Ph_2PCH_2PPh_2)_2$ reacts with a variety of terminal acetylenes [4c,4d]. In the presence of a halide-abstracting agent such as $NaPF_6$ or $NH_4PF_6$, these reactions give vinylidene complexes, which can then be deprotonated to yield the corresponding σ-acetylide complexes. By using this method, we have synthesised a range of monochloro σ-acetylide complexes from $MCl_2(phosphine)_n$ and terminal acetylenes. The mono σ-acetylide complexes $L_nM–C≡C–R$ can be designed so that the donor metal fragment is attached at the *para* position to an electron acceptor which has an optimized conjugation length. The latter can generate a highly delocalized charge-transfer state leading to high second-order non-linear optical hyperpolarizabilities in organometallic-based complexes.

The reaction of *cis*-$[MCl_2(Ph_2PCH_2PPh_2)_2]$ (M = Ru, Os) with an excess of substituted terminal acetylenes in the presence of $NaPF_6$ gives *trans*-$[(dppm)_2ClM{=}C{=}C(H)(R)]$ complexes in good yields (Scheme 1). The vinylidene complexes are intensely coloured and exhibit strong IR $\nu_{C=C}$ bands at ca. 1610–1640 $cm^{-1}$. When the vinylidene complexes were applied to a short alumina column, deprotonation gave the corresponding Ru(II) and Os(II) σ-acetylide complexes almost quantitatively. The latter complexes show intense bands in their infrared spectra at ca. 2035–2080 $cm^{-1}$ indicative of C≡C bond formation.

The molecular structure of *trans*-$[Ru(dppm)_2Cl(–C≡C–C_6H_4–p–NO_2)]$ is shown in Fig. 1. Selected bond parameters are listed in Table 1. The crystal structure consists of discrete monomer molecules in which the ruthenium is octahedrally coordinated by the chelating bis(diphenylphosphino)methane ligands and *trans* nitrophenylacetylene and chlorine ligands. The metal to phosphorus bond lengths lie in the range of 2.332(2)–2.379(2) Å. These distances are in good agreement with those in other structurally characterized ruthenium complexes [4,5]. The metal to carbon(acetylide) bond length is 1.998(7) Å and the acetylide C≡C bond length is 1.190(8) Å. The latter are in agreement with those for previously characterized acetylide complexes of iron and ruthenium. The coordination geometry of the metal centre does not exhibit any large deviation from that expected for a regular octahedral coordination, with angles between *cis*-donor atoms ranging from 70.18(6)–96.9(2)° and those between *trans* atoms within the range 177.15(6)–177.90(6)°.

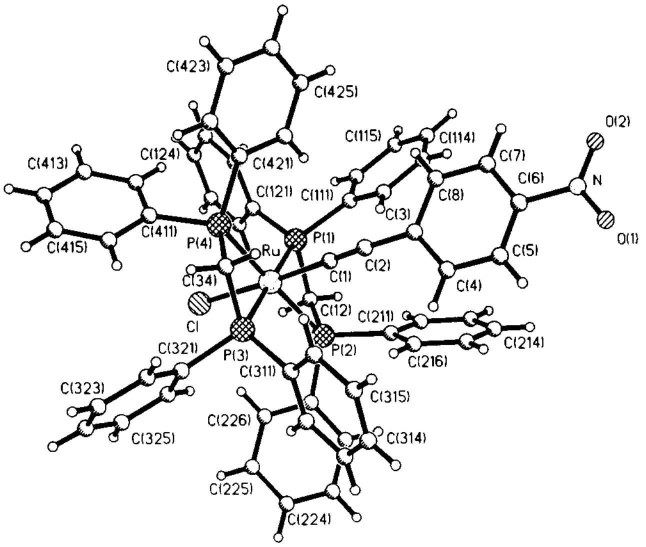

Fig. 1. Molecular structure of *trans*-$[Ru(dppm)_2Cl(–C≡C–C_6H_4–p–NO_2)]$.

Table 1
Selected bond lengths (Å) and angles (°) for *trans*-$[Ru(dppm)_2Cl(–C≡C–C_6H_4–p–NO_2)]$

| | | | |
|---|---|---|---|
| Ru–C(1) | 1.998(7) | Ru–P(3) | 2.332(2) |
| Ru–P(4) | 2.332(2) | Ru–P(2) | 2.358(2) |
| Ru–P(1) | 2.379(2) | Ru–Cl | 2.483(2) |
| P(1)–C(12) | 1.842(6) | P(2)–C(12) | 1.843(6) |
| P(3)–C(34) | 1.840(6) | P(4)–C(34) | 1.849(6) |
| C(1)–C(2) | 1.190(8) | C(2)–C(3) | 1.428(8) |
| C(3)–C(4) | 1.404(8) | C(3)–C(8) | 1.412(8) |
| C(4)–C(5) | 1.377(8) | C(5)–C(6) | 1.358(8) |
| C(6)–C(7) | 1.367(9) | C(6)–N | 1.467(9) |
| C(7)–C(8) | 1.375(9) | N–O(2) | 1.207(8) |
| N–O(1) | 1.220(8) | | |
| C(1)–Ru–P(3) | 82.0(2) | C(1)–R–P(4) | 85.0(2) |
| P(3)–Ru–P(4) | 70.98(6) | C(1)–Ru–P(2) | 92.1(2) |
| P(3)–Ru–P(2) | 108.56(6) | P(4)–Ru–P(2) | 177.15(6) |
| C(1)–Ru–P(1) | 99.6(2) | P(3)–Ru–P(1) | 177.90(6) |
| P(4)–Ru–P(1) | 110.37(6) | P(2)–Ru–P(1) | 70.18(6) |
| C(1)–Ru–Cl | 177.7(2) | P(3)–Ru–Cl | 98.44(6) |
| P(4)–Ru–Cl | 93.00(6) | P(2)–Ru–Cl | 89.85(6) |
| P(1)–Ru–Cl | 79.95(6) | C(12)–P(1)–Ru | 92.2(2) |
| C(12)–P(2)–Ru | 92.9(2) | C(34)–P(3)–Ru | 93.7(2) |
| C(34)–P(4)–Ru | 93.5(2) | C(2)–C(1)–Ru | 176.8(5) |
| C(1)–C(2)–C(3) | 168.4(7) | C(5)–C(6)–N | 119.4(7) |
| C(7)–C(6)–N | 118.1(7) | O(2)–N–O(1) | 123.9(8) |
| O(2)–N – C(6) | 118.4(8) | O(1)–N–C(6) | 117.7(8) |
| P(1)–C(12)–P(2) | 95.3(3) | P(3)–C(34)–P(4) | 94.4(3) |

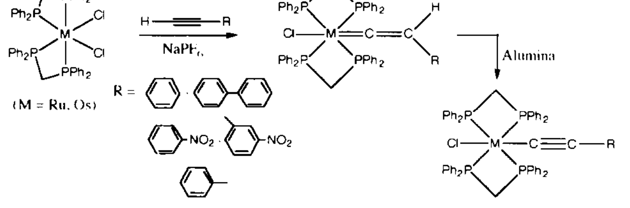

Scheme 1.

Table 2
IR $\nu_{C-C}$ stretching frequencies for various acetylide ligands and corresponding Ru and Os complexes

| Compound | IR ($\nu_{C\equiv C}$) (cm$^{-1}$) |
|---|---|
| $H–C\equiv C–C_6H_5$ | 2110 |
| $H–C\equiv C–$*p*-$C_6H_4–C_6H_5$ | 2109 |
| $H–C\equiv C–$*p*-$C_6H_4–NO_2$ | 2115 |
| $H–C\equiv C–C_6H_3$–2-$CH_2$–4-$NO_2$ | 2110 |
| $H–C\equiv C–$*p*-$C_6H_4–CH_3$ | 2107 |
| *trans*-[$(dppm)_2ClRu–C\equiv C–C_6H_5$] | 2080 |
| *trans*-[$(dppm)_2ClRu–C\equiv C–$*p*-$C_6H_4–C_6H_5$] | 2079 |
| *trans*-[$(dppm)_2ClRu–C\equiv C–$*p*-$C_6H_4–NO_2$] | 2059 |
| *trans*-[$(dppm)_2ClRu–C\equiv C–C_6H_3$–2-$(CH_3)$–4-$NO_2$] | 2050 |
| *trans*-[$(dppm)_2ClRu–C\equiv C–$*p*-$C_6H_4–CH_3$] | 2071 |
| *trans*-[$(dppm)_2ClOs–C\equiv C–C_6H_5$] | 2079 |
| *trans*-[$(dppm)_2ClOs–C\equiv C–$*p*-$C_6H_4–C_6H_5$] | 2075 |
| *trans*-[$(dppm)_2ClOs–C\equiv C–$*p*-$C_6H_4–NO_2$] | 2055 |
| *trans*-[$(dppm)_2ClOs–C\equiv C–C_6H_3$–2-$(CH_3)$–4-$NO_2$] | 2035 |
| *trans*-[$(dppm)_2ClOs–C\equiv C–$*p*-$C_6H_4–CH_3$] | 2080 |

An assessment of conjugation in the metal–acetylide complexes may be obtained from their $\nu_{C\equiv C}$ stretching frequencies in the IR spectra. We expect conjugation to be enhanced in a complex containing terminal donor–acceptor groups. A comparison of the data presented in Table 2 indicates that there is a significant downfield shift in the $\nu_{C\equiv C}$ stretching frequencies for the complexes *trans*-[$M(dppm)_2Cl(–C\equiv C–C_6H_4$-*p*-$NO_2$)] compared will those for complexes without electron-withdrawing groups at the *para* positions. For the former complexes, the $\nu_{C\equiv C}$ stretching frequencies are 20–35 wavenumbers lower, possibly suggesting stronger metal-to-acetylide bonding in such complexes. The nitro group attached at the *para* position enhances the metal-to-acetylide ligand electron donation and hence increases conjugation along the backbone. This also suggests that the donor (metal) and the acceptor ($NO_2$) groups communicate with each other through the acetylenic linkage. Such an interaction is expected to lead to higher values of the second-order non-linear optical molecular polarizability, $\beta$.

In conclusion, we have prepared a series of asymmetrically substituted vinylidene and $\sigma$-acetylide complexes of ruthenium(II) and osmium(II). The latter represent the first known examples of Os(II) vinylidene and mono-$\sigma$-acetylide complexes. We are currently investigating the detailed linear and non-linear optical properties of these complexes.

## 3. Experimental details

All experiments were performed under nitrogen by use of standard Schlenk line techniques. Solvents were predried and distilled from appropriate drying agents. Solution infrared spectra were recorded on a Perkin-Elmer 1710 Fourier-Transform IR spectrometer. $^1H$ and $^{31}P$ NMR spectra were recorded on a Bruker AM-400 spectrometer. The $^{31}P$ NMR chemical shifts are reported downfield from external trimethylphosphite standard. Microanalyses were carried out at the University Chemical Laboratory (Cambridge), and the mass spectra were recorded on a Kratos MS60 spectrometer. The metal chloride salts *cis*-[$MCl_2(dppm)_2$] (M = Ru, Os) were prepared by published methods [6]. The derivatives of phenylacetylene were synthesized by published procedures [7].

### 3.1. Syntheses

### 3.1.1. Vinylidene complexes

The vinylidene complexes were prepared by a general procedure as outlined below for *trans*-[$(dppm)_2ClOs{=}C{=}C(H)(C_6H_4$-*p*-$NO_2$)]$PF_6$. To the pale yellow solution of 20 mg ($1.94\times10^{-5}$ mol) of *cis*-[$Os(dppm)_2Cl_2$] in 30 ml of dichloromethane were added 14 mg ($9.71\times10^{-5}$ mol) of *para*-nitrophenylacetylene and 6.5 mg ($3.88\times10^{-5}$ mol) of sodium hexafluorophosphate. After 4 h, the solvent was removed in vacuo from the deep yellow solution. The resulting yellow solid was washed with 3 × 30 ml of hexane and recrystallised from dichloromethane/hexane (1 : 1) mixture to give yellow crystals.

### 3.1.2. σ-Acetylide complexes

All $\sigma$-acetylide complexes reported herein were prepared from the corresponding vinylidene complexes. The vinylidene complexes were dissolved in dichloromethane and applied to a short alumina column. Elution with dichloromethane afforded the acetylide complexes in quantitative yield.

[$(Ph_2PCH_2PPh_2)_2ClRu{=}C{=}C(H)(C_6H_5)$]$PF_6$: Orange solid. FAB MS: 1007 (calc., 1007; $M^+ - PF_6^-$). Anal. Calc. for $C_{58}H_{50}P_5ClF_6Ru$: C, 60.45; H, 4.37%. Found: C, 60.78; H, 4.39%. IR ($CH_2Cl_2$) ($\nu_{C=C}$) (cm$^{-1}$): 1631. $^{31}P\{^1H\}$ ($CDCl_3$, 250 MHz) $\delta$: −155.2 (s) ppm.

[$(Ph_2PCH_2PPh_2)_2ClRu{=}C{=}C(H)($*p*-$C_6H_4$-$C_6H_5$)]$PF_6$: Yellow solid. FAB MS: 1084 (calc., 1083; $M^+ - PF_6^-$). Anal. Calc. for $C_{64}H_{54}P_5ClF_6Ru$: C, 62.57; H, 4.43%. Found: C, 62.67; H, 4.47%. IR ($CH_2Cl_2$) ($\nu_{C=C}$) (cm$^{-1}$): 1639. $^{31}P\{^1H\}$ ($CDCl_3$, 250 MHz) $\delta$: −155.3 (s) ppm.

[$(Ph_2PCH_2PPh_2)_2ClRu{=}C{=}C(H)$-*p*-$C_6H_4$-$NO_2$]$PF_6$: Orange solid. FAB MS: 1052 (calc., 1052; $M^+ - PF_6^-$). Anal. Calc. for $C_{58}H_{49}NO_2P_5ClF_6Ru$: C, 58.28; H, 4.19; N, 1.11%. Found: C, 58.18; H, 4.12; N, 1.17%. IR ($CH_2Cl_2$) ($\nu_{C=C}$) (cm$^{-1}$): 1640. $^{31}P\{^1H\}$ ($CDCl_3$, 250 MHz) $\delta$: −155.2 (s) ppm.

[$(Ph_2PCH_2PPh_2)_2ClRu{=}C{=}C{=}(H)$-*p*-$C_6H_4$-$CH_3$]$PF_6$: Beige solid. FAB MS: 1021 (calc., 1021; $M^+ - PF_6^-$). Anal. Calc. for $C_{59}H_{52}P_5ClF_6Ru$: C, 60.75; H, 4.49%; Found: C, 60.79; H, 4.49%. IR ($CH_2Cl_2$)

Table 3
Atomic coordinates ($\times 10^4$) and equivalent isotropic displacement parameters (Å$^2$ $\times 10^3$) for trans-[Ru(dppm)$_2$Cl(–C≡C–C$_6$H$_4$-$p$-NO$_2$)]

| Atom | $x$ | $y$ | $z$ | $U_{eq}$ [a] |
|---|---|---|---|---|
| Ru | 2140(1) | 624(1) | 1770(1) | 33(1) |
| Cl | 1468(1) | −1229(2) | 1987(1) | 50(1) |
| P(1) | 2654(1) | −766(2) | 1142(1) | 39(1) |
| P(2) | 3149(1) | −240(2) | 2204(1) | 38(1) |
| P(3) | 1636(1) | 1931(2) | 2411(1) | 37(1) |
| P(4) | 1175(1) | 1565(2) | 1332(1) | 36(1) |
| C(1) | 2655(3) | 2124(6) | 1568(2) | 35(2) |
| C(2) | 2933(3) | 3050(6) | 1454(2) | 43(2) |
| C(3) | 3387(3) | 4009(5) | 1299(3) | 42(2) |
| C(4) | 3723(3) | 4763(6) | 1700(3) | 50(2) |
| C(5) | 4203(3) | 5625(6) | 1555(3) | 55(2) |
| C(6) | 4346(3) | 5749(6) | 1001(3) | 56(2) |
| C(7) | 4025(4) | 5067(6) | 587(3) | 67(2) |
| C(8) | 3545(4) | 4204(6) | 729(3) | 58(2) |
| N | 4875(4) | 6628(7) | 836(4) | 85(2) |
| O(1) | 5102(3) | 7327(6) | 1196(3) | 112(2) |
| O(2) | 5051(4) | 6635(6) | 352(3) | 127(3) |
| C(12) | 3129(3) | −1549(6) | 1724(2) | 47(2) |
| C(34) | 1158(3) | 2797(5) | 1858(2) | 37(2) |
| C(111) | 3309(3) | −397(6) | 625(2) | 42(2) |
| C(112) | 3562(3) | 769(7) | 588(3) | 56(2) |
| C(113) | 4020(4) | 1079(7) | 175(3) | 64(2) |
| C(114) | 4222(4) | 238(8) | −210(3) | 63(2) |
| C(115) | 3983(4) | −909(8) | −174(3) | 74(2) |
| C(116) | 3522(4) | −1237(7) | 240(3) | 64(2) |
| C(121) | 2145(3) | −1893(6) | 752(3) | 42(2) |
| C(122) | 2169(4) | −3127(6) | 852(3) | 59(2) |
| C(123) | 1797(4) | −3935(6) | 515(3) | 71(2) |
| C(124) | 1387(4) | −3510(7) | 73(3) | 72(2) |
| C(125) | 1348(4) | −2305(7) | −35(3) | 69(2) |
| C(126) | 1723(3) | −1493(6) | 299(3) | 56(2) |
| C(211) | 3992(3) | 481(6) | 2113(2) | 42(2) |
| C(212) | 4552(4) | −122(7) | 1889(3) | 63(2) |
| C(213) | 5175(4) | 460(11) | 1817(4) | 94(3) |
| C(214) | 5258(4) | 1630(10) | 1976(4) | 86(3) |
| C(215) | 4721(4) | 2242(8) | 2207(3) | 76(2) |
| C(216) | 4088(3) | 1665(6) | 2278(3) | 56(2) |
| C(221) | 3203(3) | −779(6) | 2935(2) | 46(2) |
| C(222) | 3708(4) | −396(8) | 3312(3) | 86(3) |
| C(223) | 3680(5) | −719(9) | 3880(3) | 115(4) |
| C(224) | 3160(6) | −1396(8) | 4059(3) | 97(3) |
| C(225) | 2658(5) | −1824(8) | 3692(3) | 85(3) |
| C(226) | 2685(4) | −1509(6) | 3125(3) | 60(2) |
| C(311) | 2170(3) | 2986(6) | 2833(3) | 44(2) |
| C(312) | 2551(4) | 2516(8) | 3289(3) | 70(2) |
| C(313) | 2984(4) | 3275(11) | 3622(4) | 95(3) |
| C(314) | 3017(5) | 4465(12) | 3481(4) | 98(4) |
| C(315) | 2652(4) | 4948(8) | 3035(4) | 83(3) |
| C(316) | 2224(4) | 4194(7) | 2702(3) | 61(2) |
| C(321) | 970(3) | 1444(6) | 2897(2) | 35(2) |
| C(322) | 431(3) | 2180(6) | 3052(2) | 49(2) |
| C(323) | −84(3) | 1755(7) | 3392(3) | 59(2) |
| C(324) | −61(4) | 589(8) | 3580(3) | 56(2) |
| C(325) | 480(4) | −150(7) | 3447(3) | 58(2) |
| C(326) | 996(3) | 276(6) | 3106(2) | 47(2) |
| C(411) | 300(3) | 916(5) | 1294(2) | 37(2) |
| C(412) | 150(3) | 81(6) | 882(3) | 57(2) |
| C(413) | −513(4) | −412(6) | 813(3) | 63(2) |
| C(414) | −1020(4) | −91(7) | 1171(3) | 66(2) |
| C(415) | −880(4) | 728(8) | 1586(3) | 69(2) |
| C(416) | −218(3) | 1229(7) | 1652(3) | 59(2) |
| C(421) | 1210(3) | 2278(5) | 642(2) | 36(2) |
| C(422) | 654(3) | 2950(5) | 417(2) | 45(2) |
| C(423) | 689(4) | 3466(6) | −112(3) | 55(2) |
| C(424) | 1274(4) | 3336(6) | −417(3) | 60(2) |
| C(425) | 1830(4) | 2680(7) | −199(3) | 60(2) |
| C(426) | 1799(3) | 2150(6) | 329(3) | 46(2) |

[a] $U_{(eq)}$ is defined as one-third of the trace of the orthogonalized $U_{ij}$ tensor.

($\nu_{C=C}$) (cm$^{-1}$): 1645. $^{31}$P{$^1$H} (CDCl$_3$, 250 MHz) δ: −155.3 (s) ppm.

[(Ph$_2$PCH$_2$PPh$_2$)$_2$ClRu=C=C=(H)C$_6$H$_3$-2-(CH$_3$)-4-NO$_2$)]PF$_6$: Orange solid. FAB MS: 1066 (calc., 1066; M$^+$− PF$_6^-$). Anal. Calc. for C$_{59}$H$_{51}$NO$_2$P$_5$ClF$_6$Ru: C, 58.49; H, 4.24 N, 1.16%; Found: C, 58.88; H, 4.28; N, 1.15%. IR (CH$_2$Cl$_2$) ($\nu_{C=C}$) (cm$^{-1}$): 1637. $^{31}$P{$^1$H} (CDCl$_3$, 250 MHz) δ: −155.2 (s) ppm.

[(Ph$_2$PCH$_2$PPh$_2$)$_2$ClRu-C≡C-$p$-C$_6$H$_5$]: Yellow solid. FAB MS: 1006 (calc., 1006). Anal. Calc. for C$_{58}$H$_{49}$P$_4$ClRu: C, 69.21; H, 4.90%; Found: C, 69.53; H, 4.81%. $^{31}$P{$^1$H} (CDCl$_3$, 250 MHz) δ: −147.4 (s) ppm.

[(Ph$_2$PCH$_2$PPh$_2$)$_2$ClRu-C≡C-$p$-C$_6$H$_4$-C$_6$H$_5$]: Yellow solid. FAB MS: 1082 (calc., 1082). Anal. Calc. for C$_{64}$H$_{53}$P$_4$ClRu: C, 71.00; H, 4.93%; Found: C, 70.89; H, 4.93%. $^{31}$P{$^1$H} (CDCl$_3$, 250 MHz) δ: −147.5 (s) ppm.

[(Ph$_2$PCH$_2$PPh$_2$)$_2$ClRu-C≡C-$p$-C$_6$H$_4$-NO$_2$]: Red solid. FAB MS: 1052 (calc., 1051). Anal. Calc. for C$_{58}$H$_{48}$NO$_2$P$_4$ClRu: C, 66.25; H, 4.60; N, 1.33%. Found: C, 66.80; H, 4.54; N, 1.27%. $^{31}$P{$^1$H} (CDCl$_3$, 250 MHz) δ: −148.0 (s) ppm.

[(Ph$_2$PCH$_2$PPh$_2$)$_2$ClRu-C≡C-C$_6$H$_3$-2-(CH$_3$)-4-NO$_2$]: Red solid. FAB MS: 1066 (calc., 1065). Anal. Calc. for C$_{59}$H$_{50}$NO$_2$P$_4$ClRu: C, 66.51; H, 1.31%. Found: C, 65.91; H, 4.81%. $^{31}$P{$^1$H} (CDCl$_3$, 250 MHz) δ: −147.6 (s) ppm.

[(Ph$_2$PCH$_2$PPh$_2$)$_2$ClRu-C≡C-$p$-C$_6$H$_4$-CH$_3$]: Yellow solid. FAB MS: 1022 (calc., 1020). Anal. Calc. for C$_{59}$H$_{51}$P$_4$ClRu: C, 69.44; H, 5.04%. Found: C, 69.28; H, 5.04%. $^{31}$P{$^1$H} (CDCl$_3$, 250 MHz) δ: −148.9 (s) ppm.

[(Ph$_2$PCH$_2$PPh$_2$)$_2$ClOs=C=C—(H)(C$_6$H$_5$)]PF$_6$: Pink solid. FAB MS: 1095 (calc., 1096; M$^+$− PF$_6^-$) Anal. Calc. for C$_{58}$H$_{50}$P$_5$ClF$_6$Os: C, 56.11; H, 4.06%. Found: C, 56.16; H, 4.06%. IR (CH$_2$Cl$_2$) ($\nu_{C=C}$) (cm$^{-1}$): 1636. $^{31}$P{$^1$H} (CDCl$_3$, 250 MHz) δ: −194.1 (s) ppm.

[(Ph$_2$PCH$_2$PPh$_2$)$_2$ClOs=C=C-(H)($p$-C$_6$H$_4$-C$_6$H$_5$)]PF$_6$: Pink solid. FAB MS: 1173 (calc., 1173; M$^+$− PF$_6^-$). Anal. Calc. for C$_{64}$H$_{54}$P$_5$ClF$_6$Os: C, 58.34; H, 4.13%. Found: C, 58.27; H, 4.26%. IR (CH$_2$Cl$_2$) ($\nu_{C=C}$) (cm$^{-1}$): 1642. $^{31}$P{$^1$H} (CDCl$_3$, 250 MHz) δ: −193.0 (s) ppm.

$[(Ph_2PCH_2PPh_2)_2ClOs{=}C{=}C{-}(H)(p{-}C_6H_4{-}NO_2)]PF_6$: Orange solid. FAB MS: 1142 (calc., 1142; $M^+ - PF_6^-$). Anal. Calc. for $C_{58}H_{49}NO_2P_5ClF_6Os$: C, 54.14; H, 3.84%. Found: C, 54.40; H, 3.81% IR ($CH_2Cl_2$) ($\nu_{C=C}$) ($cm^{-1}$): 1607. $^{31}P\{^1H\}$ ($CDCl_3$, 250 MHz) $\delta$: $-195.2$ (s) ppm.

$[(Ph_2PCH_2PPh_2)_2ClOs{=}C{=}C{-}(H){-}p{-}C_6H_4{-}CH_3]PF_6$: Pink solid. FAB MS: 1112 (calc., 1111; $M^+ - PF_6^-$). Anal. Calc. for $C_{59}H_{52}P_5F_6ClOs$: C, 56.44; H, 4.17%. Found: C, 56.78; H, 4.19%. IR ($CH_2Cl_2$) ($\nu_{C=C}$) ($cm^{-1}$): 1647. $^{31}P\{^1H\}$ ($CDCl_3$, 250 MHz) $\delta$: $-193.384$ (s) ppm.

$[(Ph_2PCH_2PPh_2)_2ClOs{=}C{=}C{-}(H)(C_6H_2{-}2{-}(CH_3){-}4{-}NO_2)]PF_6$: Orange solid. FAB MS: 1156 (calc., 1156; $M^+ - PF_6^-$). Anal. Calc. for $C_{59}H_{51}NO_2P_5F_6ClOs$: C, 54.49; H, 3.95; N, 1.08%. Found: C, 54.24; H, 4.01; N, 1.19%. IR ($CH_2Cl_2$) ($\nu_{C=C}$) ($cm^{-1}$): 1638. $^{31}P\{^1H\}$ ($CDCl_3$, 250 MHz) $\delta$: $-195.1$ (s) ppm.

$[(Ph_2PCH_2PPh_2)_2ClOs{-}C{\equiv}C{-}p{-}C_6H_5]$: Yellow solid. FAB MS: 1095 (calc., 1095). Anal. Calc. for $C_{58}H_{49}P_4ClOs$: C, 60.65; H, 4.98%. Found: C, 63.59; H, 4.48%. $^{31}P\{^1H\}$ ($CDCl_3$, 250 MHz) $\delta$: $-193.3$ (s) ppm.

$[(Ph_2PCH_2PPh_2)_2ClOs{-}C{\equiv}C{-}p{-}C_6H_4{-}C_6H_5]$: Yellow-green solid. FAB MS: 1172 (calc., 1172). Anal. Calc. for $C_{64}H_{53}P_4ClOs$: C, 65.56; H, 4.52; P, 10.58%. Found: C, 61.07; H, 4.21; P, 1.22%. $^{31}P\{^1H\}$ ($CDCl_3$, 250 MHz) $\delta$: $-193.2$ (s) ppm.

$[(Ph_2PCH_2PPh_2)_2ClOs{-}C{\equiv}C{-}p{-}C_6H_4{-}NO_2]$: Purple solid. FAB MS: 1142 (cald., 1140). Anal. Calc. for $C_{58}H_{48}NO_2P_4ClOs$: C, 58.33; H, 4.25; P, 1.11%. Found: C, 61.07; H, 4.21; P, 1.22%. $^{31}P\{^1H\}$ ($CDCl_3$; 250 MHz) $\delta$: $-193.3$ (s) ppm.

$[(Ph_2PCH_2PPh_2)_2ClOs{-}C{\equiv}C{-}p{-}C_6H_3{-}2{-}CH_3{-}4{-}NO_2]$. Purple solid. FAB MS: 1156 (calc., 1154). Anal. Calc. for $C_{59}H_{50}NO_2P_4ClOs$: C, 61.37; H, 4.36; N, 1.21%. Found: C, 60.78; H, 4.39; N, 1.18%. $^{31}P\{^1H\}$ ($CDCl_3$, 250 MHz) $\delta$: $-193.3$ (s) ppm.

$[(Ph_2PCH_2PPh_2)_2ClOs{-}C{\equiv}C{-}p{-}C_6H_4{-}CH_3]$. Pink solid. FAB MS: 1112 (calc., 1110). Anal. Calc. for $C_{59}H_{51}P_4ClOs$: C, 63.86; H, 4.63%. Found: C, 63.23; H, 4.69%. $^{31}P\{^1H\}$ ($CDCl_3$, 250 MHz) $\delta$: $-193.4$ (s) ppm.

### *3.2. X-Ray data collection, structure solution and refinement summary for trans-*$\{[(C_6H_5)_2PCH_2P(C_6H_5)_2]_2Cl{-}Ru{-}C{\equiv}C{-}C_6H_4{-}p{-}NO_2\}$

The crystals were grown by two-layer crystallisation from dichloromethane/hexane (1:1). Crystal data: $C_{58}H_{48}P_4O_2NClRu$, $M = 1051.37$, space group $P2_1/c$, $a = 19.149(5)$, $b = 11.062(3)$, $c = 23.711(7)$ Å, $\beta = 92.07(2)°$, $V = 5020(2)$ Å$^3$, $Z = 4$, $D_c = 1.391$ g cm$^{-3}$, $F(000) = 2160$, $\mu(\text{Mo K}\alpha) = 0.537$ mm$^{-1}$.

A red block-shaped crystal of approximate dimensions $0.20 \times 0.20 \times 0.30$ mm was mounted on a glass fibre; $D_0$ was not recorded, accurate lattice parameters were determined from 30 reflections ($\theta = 12.02$–$13.41°$). Intensity data were measured on a Nicolet P3 diffractometer, using monochromated Mo K$\alpha$ radiation and a $\sigma$ scan mode to a maximum value for $\theta$ of 22.54°. Three standard reflections were monitored every 97 reflections collected and showed no significant decrease in standard intensity during the data collection time. A total of 7032 reflections were measured within the range of $0 < h < 20$, $0 < k < 11$, $-25 < l < 25$ and averaged to yield 6575 unique reflections ($R_{int} = 0.0227$) of which 4174 were judged as significant by the criterion $F_{obs} > 4\sigma(F_{obs})$. Corrections were applied for Lorentz and polarisation effects. Absorption corrections were also applied by the use of semi-empirical $\psi$ scans (minimum and maximum transmission coefficients of 0.070 and 0.0966, respectively).

Structure solution was by a combination of Patterson methods and Fourier techniques. Anisotropic thermal motion was assumed for all non-hydrogen atoms. Full matrix least-squares refinement on $F_{obs}^2$ for 6574 data and 614 parameters converged to $R_w^2 = 0.0966$ (all data), conventional $R = 0.0513$ (observed data). $(\Delta/\sigma)_{max} = -0.001$. GOF (all data) = 1.072. The function minimised was $\Sigma w(F_{obs}^2 - F_{calc}^2)^2$, $w = 1/[2(F_{obs}^2) + (0.0293P)^2 + 0.0667P]$ where $P = (F_{obs}^2 + 2F_{calc}^2)/3$ and $\sigma$ was obtained from counting statistics. A final difference electron density Fourier synthesis revealed maximum and minimum electron density peaks of 0.330 and $-0.296$ e A$^{-3}$. Atomic coordinates for the non-hydrogen atoms and their equivalent isotropic displacement parameters are listed in Table 3.

Tables of hydrogen atom coordinates and thermal parameters, and a full list of bond lengths and angles have been deposited at the Cambridge Crystallographic Data Centre.

## Acknowledgements

We thank the EPSRC (A.J.H., S.L.I., M.S.K.), ICI (A.J.H.), Kobe Steel Europe Ltd. (M.S.K.) and Darwin College, Cambridge (N.J.L.) for financial assistance.

## References

[1] (a) J. Zyss (ed.), *Molecular Nonlinear Optics: Materials, Physics, and Devices*, Academic Press, Boston, MA 1993; (b) N.P. Prasad and D.J. Williams, *Introduction to Nonlinear Optical Effects in Molecules and Polymers*, Wiley, New York, 1991; (c) R.A. Hann and D. Bloor (eds.), *Organic Materials for Nonlinear Optics II*, Royal Society of Chemistry, London, 1991.

[2] (a) S.R. Marder, J.W. Perry, B.G. Tiemann and W.P. Schaefer, *Organometallics, 10* (1991) 1896; (b) S.R. Marder, J.E. Sohn and G.D. Stucky (eds.), *Materials for Nonlinear Optics: Chemical Perspectives, ACS Symp. Ser. No. 455*, Am. Chem. Soc., Washington, DC, 1991; (c) T.M. Gilbert, F.J. Hadley, C.B. Bauer and R.D. Rogers, *Organometallics, 13* (1994) 2024.

[3] T.B. Marder, G. Lesley, Z. Yuan, H.B. Fyfe, P. Chow, G. Stringer, I.R. Jobe, N.J. Taylor, I.D. Williams and S.K. Kurtz, in Ref. [2b] above, pp. 605–615.

[4] (a) M.I. Bruce and R.C. Wallis, *Aust. J. Chem., 32* (1971) 1471; (b) M.I. Bruce, F.S. Wong, B.W. Skelton and A.H. White, *J. Chem. Soc., Dalton Trans.*, (1982) 2203; (c) P. Haquette, N. Pirio, D. Touchard, L. Toupet and P.H. Dixneuf, *J. Chem. Soc., Chem. Commun.,* (1993) 163; (d) D. Touchard, C. Morice, V. Cadierno, P. Haquette, L. Toupet and P.H. Dixneuf, *J. Chem. Soc., Chem. Commun.*, (1994) 859.

[5] (a) Z. Atherton, C.W. Faulkner, S.L. Ingham, A.K. Kakkar, M.S. Khan, J. Lewis, N.J. Long and P.R. Raithby, *J. Organomet. Chem., 462* (1994) 265; (b) Y. Sun, N.J. Taylor and A.J. Carty, *Organometallics, 11* (1992) 4293; Y. Sun, N.J. Taylor and A.J. Carty, *J. Organomet. Chem., 423* (1992) C43; (c) S.L. Ingham, M.S. Khan, J. Lewis, N.J. Long and P.R. Raithby, *J. Organomet. Chem., 470* (1994) 153.

[6] J. Chatt and R.G. Hayter, *J. Chem. Soc., Dalton Trans.,* (1961) 896.

[7] M.E. Wright, *Macromolecules, 22* (1989) 3256.